Table Look-Up Estimation of Signal and Noise Parameters From Quantized Observables

V. A. Vilnrotter and E. R. Rodemich
Communications Systems Research Section

In this article we examine a table look-up algorithm for estimating underlying signal and noise parameters from quantized observables. A general mathematical model is developed, and a look-up table designed specifically for estimating parameters from four-bit quantized data is described. Estimator performance is evaluated both analytically and by means of numerical simulation, and an example is provided to illustrate the use of the look-up table for estimating signal-to-noise ratios commonly encountered in Voyager-type data.

I. Introduction

In this article, we consider the problem of estimating signal and noise parameters from quantized samples of an observed waveform, by means of a table look-up algorithm. The waveform consists of binary antipodal signal plus additive Gaussian noise. The justification for the look-up table approach hinges on the observation that if the parameters of interest are single-valued functions of some computable quantities associated with the samples, then it should be possible to construct a table whose entries at the appropriate coordinates are the desired parameter estimates. Indeed, we shall show that for the class of problems under consideration, the first two absolute moments of the quantized samples can serve as entry coordinates to a two-dimensional look-up table. Thus, the problem reduces to that of finding accurate estimates for the first two absolute moments. Since accurate estimates of the required absolute moments can usually be found (as long as a large number of independent samples are available), the table look-up algorithm may often be employed to obtain quick and accurate parameter estimates.

The above approach was originally suggested to the authors by W. J. Hurd of the Communications Systems Research Section and was used in non-real-time symbol-stream combining of Voyager telemetry data (Ref. 1). In the following sections, suitable mathematical models are developed and employed to evaluate estimator performance. An example is provided to illustrate the use of the look-up table for estimating signal-to-noise ratios in data streams typical of actual Voyager data.

II. Estimator Model

The table look-up algorithm may be used to estimate signal amplitude and noise standard deviation from a sequence of random variables obtained by synchronously integrating the received noise-corrupted waveform over the duration of each binary symbol. Thus, if the received waveform is expressed as

$$r(t) = D(t)\,(A/T) + n(t) \qquad (1)$$

(where A is the integrated symbol amplitude and $n(t)$ is additive Gaussian noise) then synchronous T-second integration over the ith symbol interval yields

$$r_i = \int_{(i-1)T}^{iT} r(t)\,dt = D_i A + n_i \tag{2}$$

where D_i is the integral of the antipodal modulation $D(t)$ (hence D_i takes on the value ±1 with probability P_1 and P_{-1}, respectively) and the noise samples n_i are assumed to be independent, zero-mean Gaussian random variables with variance σ^2. The probability density of each sample can be found by averaging the conditional densities (conditioned on the data) over the a priori statistics of D_i. Assuming stationary statistics we can suppress the subscript "i" and write

$$\begin{aligned} p_r(R) &= P_1 p_r(R \mid D = 1) + P_{-1} p_r(R \mid D = -1) \\ &= (2\pi\sigma^2)^{-1/2} \left\{ P_1\, e^{-(R-A)^2/2\sigma^2} + P_{-1}\, e^{-(R+A)^2/2\sigma^2} \right\} \end{aligned} \tag{3}$$

Consider the case where the time samples are subjected to L-bit quantization prior to processing. In particular, let the quantized samples q take on integer values in the range

$$-2^{(L-1)} \leqslant q \leqslant 2^{(L-1)} - 1 \tag{4}$$

and let the probability that q takes on the integer value j be denoted p_j for any i:

$$p_j = \begin{cases} \displaystyle\int_j^{j+1} p_r(R)\,dR; & -2^{(L-1)} + 1 \leqslant j \leqslant 2^{(L-1)} - 2 \\ \displaystyle\int_{2^{(L-1)}_{-1}}^{\infty} p_r(R)\,dR; & j = -2^{(L-1)} \text{ or } 2^{(L-1)} - 1 \end{cases} \tag{5}$$

In typical applications the a priori probabilities of the data symbols are equal ($P_1 = P_{-1}$), in which case the quantization probabilities may be expressed as

$$p_j = \begin{cases} G(j) - G(j+1); & -2^{(L-1)} + 1 \leqslant j \leqslant 2^{(L-1)} - 2 \\ G(j); & j = -2^{(L-1)} \text{ or } 2^{(L-1)} - 1 \end{cases} \tag{6a}$$

where

$$G(j) = \frac{1}{4}\left\{ \operatorname{Erfc}\left(\frac{j-A}{\sqrt{2}\sigma}\right) + \operatorname{Erfc}\left(\frac{j+A}{\sqrt{2}\sigma}\right) \right\} \tag{6b}$$

and

$$\operatorname{Erfc}(\gamma) = \frac{2}{\sqrt{\pi}} \int_{\gamma}^{\infty} e^{-y^2}\,dy \tag{6c}$$

It is desired to obtain estimates of the parameters A and σ (denoted $\hat{A}$ and $\hat{\sigma}$) from the sample absolute mean θ_1 and sample mean-square θ_2, which are defined as

$$\theta_1 = \frac{1}{N} \sum_{i=1}^{N} |q_i| \tag{7a}$$

$$\theta_2 = \frac{1}{N} \sum_{i=1}^{N} q_i^2 \tag{7b}$$

where N is the number of samples observed. Since the quantized observables are random variables, the absolute moment vector $\boldsymbol{\theta} \triangleq (\theta_1, \theta_2)$ is a random vector whose statistics depend on the number of quantization intervals and on the total number of samples as well as on the signal and noise parameters embedded in the received waveform.

Under the assumption that a large number of independent samples are used, the joint distribution of $\boldsymbol{\theta}$ can be determined by means of the multivariate central limit theorem (Refs. 2, 3). Defining the components of the auxiliary random vector $\mathbf{x}$ as

$$x_1 = |q| - \overline{|q|} \tag{8a}$$

$$x_2 = q^2 - \overline{q^2} \tag{8b}$$

and forming the sum

$$\mathbf{z} = \frac{1}{\sqrt{N}} \sum_{i=1}^{N} \mathbf{x}_i \tag{9}$$

it follows that as N grows without bound, the distribution function of z approaches that of a jointly Gaussian random vector with covariance matrix

$$\Lambda_z = E\,[\mathbf{z}^T\mathbf{z}] = E\,[\mathbf{x}^T\mathbf{x}] = \Lambda_x \tag{10}$$

where, for any i, the components of Λ_x are

$$\lambda_{11} = E(x_1^2) = \overline{q^2} - (\overline{|q|})^2 \tag{11a}$$

$$\lambda_{12} = \lambda_{21} = E(x_1 x_2) = \overline{|q|^3} - \overline{|q|}\,\overline{q^2} \tag{11b}$$

$$\lambda_{22} = E(x_2^2) = \overline{q^4} - (\overline{q^2})^2 \tag{11c}$$

Here, as well as in equations (8), the overbar denotes expectation. The kth absolute moment is defined as

$$\overline{|q|^k} = \sum_j |j|^k p_j \tag{12}$$

Since the absolute moment vector can be expressed as

$$\boldsymbol{\theta} = \frac{1}{\sqrt{N}}\mathbf{z} + \bar{\boldsymbol{\theta}} \tag{13a}$$

$$\bar{\boldsymbol{\theta}} = (\overline{|q|}, \overline{q^2}) \tag{13b}$$

The central limit theorem implies that for sufficiently large N, $\boldsymbol{\theta}$ may be modeled as a Gaussian random vector with mean value vector $\bar{\boldsymbol{\theta}}$ and covariance matrix

$$\Lambda_\theta = \frac{1}{N}\Lambda_x \tag{14}$$

Observe that as N approaches infinity, each component of Λ_θ approaches zero, implying that for any choice of input parameters and quantization levels $\boldsymbol{\theta}$ approaches the associated mean value vector $\bar{\boldsymbol{\theta}}$. It is this property of the absolute moment vector that originally motivated the construction of a table look-up algorithm for estimating signal and noise parameters.

A look-up table may be constructed in the following manner. Given L, the mean value vector $\bar{\boldsymbol{\theta}}$ may be determined for any choice of (A,σ), using equation (12), and a dense matrix generated for each component of $\bar{\boldsymbol{\theta}}$ over the desired range of A and σ. Numerical interpolation then enables one to compute estimates of A and σ corresponding to a uniformly spaced grid over $(\bar{\theta}_1, \bar{\theta}_2)$.

In the current application, a look-up table was constructed for obtaining the estimates $(\hat{A},\hat{\sigma})$ from four-bit quantized samples ($L = 4$), over the range $0.5 \leqslant (A,\sigma) \leqslant 5.5$. It was useful to introduce the predistortion transformation $(\theta_1, \theta_2) \rightarrow (\theta_1, \Theta)$ where

$$\Theta = [\max(0., 1.39211 - 0.0519\,\theta_1 - (\sqrt{\theta_2}/\theta_1))]^{1/2} \tag{15}$$

in order to improve resolution over certain regions of interest. A graphical representation of the resulting look-up table is shown in Fig. 1, illustrating the functional dependence of the parameter estimates on the transformed coordinates (θ_1, Θ). Note that some regions in the (θ_1, Θ) plane fall outside the range of the look-up table. In general, points within these external regions may be assigned special values (i.e. negative values) to distinguish them from valid parameter estimates. The user may then invoke a different estimator, or take other appropriate action, when one of these special values is encountered. In our case, the estimates depend on whether Θ is less than or greater than 0.3:

$$\Theta > 0.3; \quad \begin{cases} \hat{A} = \theta_1 \\ \hat{\sigma} = 0.5 \end{cases} \tag{16a}$$

$$\Theta \leqslant 0.3; \quad \begin{cases} \hat{A} = 0.4 \\ \hat{\sigma} = \theta_1 \sqrt{\pi/2} \end{cases} \tag{16b}$$

Given measured values of θ_1 and Θ falling within the range of the look-up table, the table entry coordinates are the integers $I\theta_1$ and $I\Theta$ most nearly satisfying

$$\theta_1 = 0.05\,(I\theta_1 + 19) \tag{17a}$$

$$\Theta = 0.005\,(I\Theta - 1) \tag{17b}$$

with $1 \leqslant I\Theta \leqslant 95$ and $1 \leqslant I\theta_1 \leqslant 81$. All table entries for A and σ were converted to integers in the range 0 to 255. Designating the integer table entries for A and σ as IA and $I\sigma$, respectively, final estimates are obtained using

$$\hat{A} = 0.4 + 0.02\,IA\,(I\theta_1, I\Theta) \tag{18a}$$

$$\hat{\sigma} = 0.4 + 0.02\,I\sigma\,(I\theta_1, I\Theta) \tag{18b}$$

Since the table entries are integers, resolution is limited to 0.02 for both estimates. Examples of the effects of this "granularity" will be provided in the next section.

III. Estimator Performance

The performance of the table look-up estimator has been evaluated both analytically and by means of numerical simula-

tion. The details of the analysis are presented in the Appendix. We shall consider the analytical results first.

A. Performance Analysis

It was shown previously that the absolute sample moment vector can be decomposed into the sum of a deterministic and a zero-mean Gaussian component, provided the total number of observed samples is sufficiently great. For convenience, represent the sample moment components as

$$\theta_1 = \bar{\theta}_1 + \alpha_1 \tag{19a}$$

$$\theta_2 = \bar{\theta}_2 + \alpha_2 \tag{19b}$$

where the mean values are defined in Eq. (13b), and (α_1, α_2) are small Gaussian random variables of mean zero and covariance matrix $\Lambda_\alpha = \Lambda_\theta$ (see Eq. [14]). The estimates $(\hat{A}, \hat{\sigma})$ are obtained by inverting the formulas for (θ_1, θ_2) in terms of A and σ. Assuming that the inverse equations can be linearized over small enough regions in the (θ_1, θ_2) plane, the estimates may also be approximated as the sum of deterministic and zero-mean Gaussian components

$$\hat{A} \simeq A + \epsilon_1 \tag{20a}$$

$$\hat{\sigma} \simeq \sigma + \epsilon_2 \tag{20b}$$

Therefore, ϵ_1 and ϵ_2 represent random estimation errors resulting from the effective additive noise components (α_1, α_2). Due to the Gaussian assumption, the error vector is completely characterized (in the statistical sense) by its covariance matrix Λ_ϵ, with components

$$\epsilon_{11} = E(\hat{A} - A)^2 \tag{21a}$$

$$\epsilon_{12} = \epsilon_{21} = E(\hat{A} - A)(\hat{\sigma} - \sigma) \tag{21b}$$

$$\epsilon_{22} = E(\hat{\sigma} - \sigma)^2 \tag{21c}$$

In order to evaluate this matrix, observe that under the linearizing approximation (which is valid for large N) the transpose of the effective noise vector can be written as

$$\alpha^T = C\epsilon^T \tag{22}$$

where C is the Jacobian of the forward transformation:

$$C = \begin{bmatrix} \dfrac{\partial\theta_1}{\partial A} & \dfrac{\partial\theta_1}{\partial\sigma} \\ \dfrac{\partial\theta_2}{\partial A} & \dfrac{\partial\theta_2}{\partial\sigma} \end{bmatrix} \tag{23}$$

An explicit calculation of the components of the Jacobian is performed in the Appendix, assuming four-bit quantization. With C^{-1} the inverse of C, the estimation error vector becomes

$$\epsilon^T = C^{-1}\alpha^T \tag{24}$$

while its covariance matrix may be represented as

$$\Lambda_\epsilon = E(\epsilon^T\epsilon) = C^{-1}\Lambda_\alpha(C^{-1})^T \tag{25}$$

This covariance matrix can be evaluated for any choice of A, σ, L and N using equations (11), (14) and (A-5). The error covariance matrix was determined at the four internal points designated in Fig. 1, namely at coordinates (2,2), (3,2), (4,2) and (3,3) in the (A, σ) domain. The results are displayed in Table 1. The expectations in Table 1 refer either to ensemble averages (obtained from the linearized analysis) or to sample averages (obtained from the simulation described in Section III.B).

B. Performance Simulation

The performance of the estimator can also be evaluated by means of numerical simulation. This can be accomplished by generating random sequences with the appropriate statistics, performing the quantization operation, taking the magnitude and square of each sample, and adding up the desired number of terms to obtain a simulated sample absolute moment vector. Next, the look-up table is entered at the coordinates specified by the components of the simulated vector, and estimates of the desired parameters are obtained. The appropriate sample statistics may be determined by repeating the above procedure a large number of times, using independent random sequences each time. However, if each random sequence consists of a large number of terms, then the multivariate central limit theorem may be invoked to generate samples of the absolute moment vector directly with the proper statistics. This latter approach was adopted in the current application.

The purpose of the simulation is to characterize estimator performance at a given value of signal level A, noise standard deviation σ, quantization level L and sample size N. Once A and σ are specified, one computes $\bar{\theta}_1 = |\bar{q}|$, $\bar{\theta}_2 = \bar{q}^2$ and simulates the noise vector α by means of the central limit theorem approximation. The simulated value of α, denoted $\tilde{\alpha}$, can be represented as a zero-mean, unit variance Gaussian random vector $\mathbf{u}$ (with independent components) scaled by a matrix Γ as

$$\tilde{\alpha} = \mathbf{u}\Gamma \tag{26}$$

where

$$\Gamma = \begin{bmatrix} \sqrt{\lambda_{11}} & , & \lambda_{12}/\sqrt{\lambda_{11}} \\ 0 & , & \sqrt{\lambda_{22} - \dfrac{\lambda_{12}^2}{\lambda_{11}}} \end{bmatrix} \frac{1}{\sqrt{N}} \tag{27}$$

It is readily verified that

$$E(\tilde{\alpha}^T\tilde{\alpha}) = \Lambda_\alpha = \Lambda_\theta \tag{28}$$

hence, in the limit of large N, the simulated approximation $\tilde{\alpha}$ has the same statistics as the actual noise vector α. The simulated sample absolute moment vector $\tilde{\theta}$ is obtained using

$$\tilde{\theta} = \bar{\theta} + \tilde{\alpha} \tag{29}$$

Next, the look-up table is entered at the coordinates specified by $\tilde{\theta}$, and the estimates $(\hat{A}, \hat{\sigma})$ recorded. This procedure is repeated K times, after which sample statistics are computed from the entries of the resulting $(2 \times K)$ array. The value $K = 10^4$ was chosen for the simulation. The distribution of the parameter estimates are displayed in Fig. 2 for typical simulation runs, using $N = 10^3$ in each case. These "scatter diagrams" serve to reveal the structure of the look-up table grid, illustrate noise-induced scattering, and indicate correlation in the estimates near the input coordinates. However, it is not possible to form an accurate mental picture of either the mean or the "spread" of the resulting sample distributions, since the number of times each visible grid point occurred is not evident. Therefore, sample statistics were computed at the four designated coordinates to provide this additional information. The simulation statistics are displayed in Table 1, directly under the analytical results. When computing these sample statistics, points that were out of range were ignored, in order to remove dependence on the choice of the ad hoc estimator employed. Most simulation runs did not register out of range points, but even when such points occurred, only a few were recorded per simulation run.

Analysis and simulation results were found to be in good agreement. Errors in the sample means were negligible, indicating that the estimates are unbiased. Discrepancies in covariance are attributed to deviation from the linear model. Indeed, by letting $N = 10^4$ at the point (3, 3), the agreement between simulation and analysis improved, as shown in the last two rows of Table 1.

C. An Application

Finally, the look-up table was employed to estimate symbol signal-to-noise ratio (SNR) for Voyager data typical of that used in the symbol stream combiner. Here symbol SNR is defined as

$$\text{SNR} = A^2/2\sigma^2 \tag{30}$$

while its estimate is obtained directly from $\hat{A}$ and $\hat{\sigma}$ as

$$\widehat{\text{SNR}} = \hat{A}^2/2\hat{\sigma}^2 \tag{31}$$

The estimator bias B, defined as

$$B = E(\widehat{\text{SNR}}) - \text{SNR} \tag{32}$$

is a measure of the difference between the mean of the estimate and the actual SNR. For an unbiased estimator, $B = 0$. Normalizing by the true SNR, one may define the ratio

$$R = E(\widehat{\text{SNR}})/\text{SNR} = 1 + \frac{B}{\text{SNR}} \tag{33}$$

which, when expressed in decibels, becomes

$$R\ (\text{dB}) = 10 \log_{10} [E(\widehat{\text{SNR}})/\text{SNR}] \tag{34}$$

(Thus, if R (dB) = 3, E(SNR) = 2 SNR, whereas if R (dB) = –3, E(SNR) = 0.5 SNR). In addition, if the bias is small compared to the true SNR, then Eq. (34) reduces to

$$R\ (\text{dB}) \simeq 10 \log_{10}(e)[B/\text{SNR}] \tag{35}$$

providing a convenient measure of the fractional bias.

The quantity R (dB) was determined by simulation for true SNRs ranging from –1 to +1 dB, and various signal levels characteristic of Voyager data. (In the simulation, expectation is approximated by the sample mean.) The number of samples used for determining each estimate was $N = 5700$ in agreement with the value used for the near-real-time symbol-stream combiner. The results, shown in Fig. 3, confirm that SNR estimates are virtually unbiased over the indicated range. The sample standard deviation of estimation error was also computed for

each signal level, and found to be nearly constant, approximately equal to 0.018 over the same range. These results indicate that the table look-up estimator examined in this article can be used to obtain unbiased estimates of symbol SNR over the range of interest for deep-space reception.

IV. Summary and Conclusions

A look-up table was constructed for the purpose of estimating signal and noise parameters from quantized samples of a noise-corrupted antipodal signal. Since the table is entered at coordinates derived from the first two sample absolute moments of the quantized observables, substantial errors in moment estimates lead directly to errors in the corresponding parameter estimates. Hence, the look-up table performs best when a large number of independent quantized samples are available to allow accurate determination of the required sample statistics. It should be observed, however, that perfect moment estimates do not necessarily yield perfect parameter estimates, due to the limited resolution inherent in any finite element table. The parameter estimates were found to be unbiased over the central region of the table, with random components that depend both on the sample size and on the spectral level of the additive noise process. Thus, the covariance matrix of the estimation error is a strong function of the coordinates at which the table is entered. It was also demonstrated that unbiased estimates of symbol SNR can be obtained, over a range of values and sample sizes characteristics of those encountered in processing actual Voyager data.

References

1. Hurd, W. J., Rabkin, J., Russell, M. D., Siev, B., Cooper, H. W., Anderson, T. O., and Winter, P. U., "Antenna Arraying of Voyager Telemetry Signals by Symbol Stream Combining," *TDA Progress Report 42–86*, Jet Propulsion Laboratory, Pasadena, Calif., pp. 131–142, Aug. 15, 1986.

2. Wozencraft, J. M., and Jacobs, I. M., *Principles of Communication Engineering*, Chapt. 3., John Wiley & Sons, New York, 1965.

3. Wilks, S. S., *Mathematical Statistics*, Chapt. 9, John Wiley & Sons, New York, 1962.

Table 1. Comparison of analysis and simulation results

	$E(\hat{A})$	$E(\hat{\sigma})$	$E(\hat{A}\text{-}\bar{\hat{A}})^2$	$E(\hat{A}\text{-}\bar{\hat{A}})\,(\hat{\sigma}\text{-}\bar{\hat{\sigma}})$	$E(\hat{\sigma}\text{-}\bar{\hat{\sigma}})^2$
$N = 10^3$					
Analysis	2.0	2.0	1.258×10^{-2}	-8.370×10^{-3}	1.089×10^{-2}
Simulation	1.988	2.008	1.578×10^{-2}	-9.995×10^{-3}	1.206×10^{-2}
Analysis	3.0	2.0	5.242×10^{-3}	-1.390×10^{-3}	4.783×10^{-3}
Simulation	2.998	2.002	5.606×10^{-3}	-1.428×10^{-3}	5.159×10^{-3}
Analysis	4.0	2.0	4.535×10^{-3}	-1.640×10^{-4}	3.562×10^{-3}
Simulation	4.001	1.997	5.640×10^{-3}	7.2×10^{-5}	3.572×10^{-3}
Analysis	3.0	3.0	2.889×10^{-2}	-2.379×10^{-2}	3.640×10^{-2}
Simulation	2.967	3.024	4.344×10^{-2}	-3.429×10^{-2}	4.375×10^{-2}
$N = 10^4$					
Analysis	3.0	3.0	2.889×10^{-3}	-2.379×10^{-3}	3.640×10^{-3}
Simulation	2.996	3.002	3.651×10^{-3}	-2.623×10^{-3}	3.509×10^{-3}

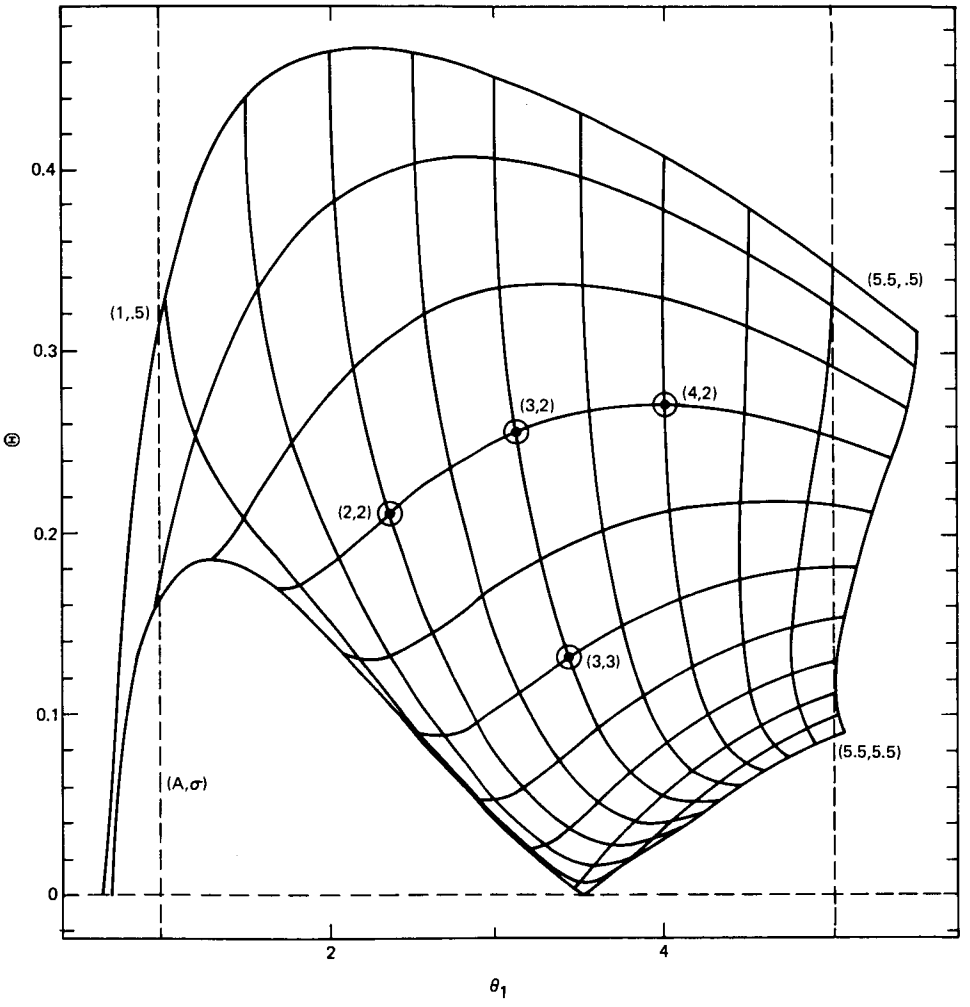

Fig. 1. Look-up table representation

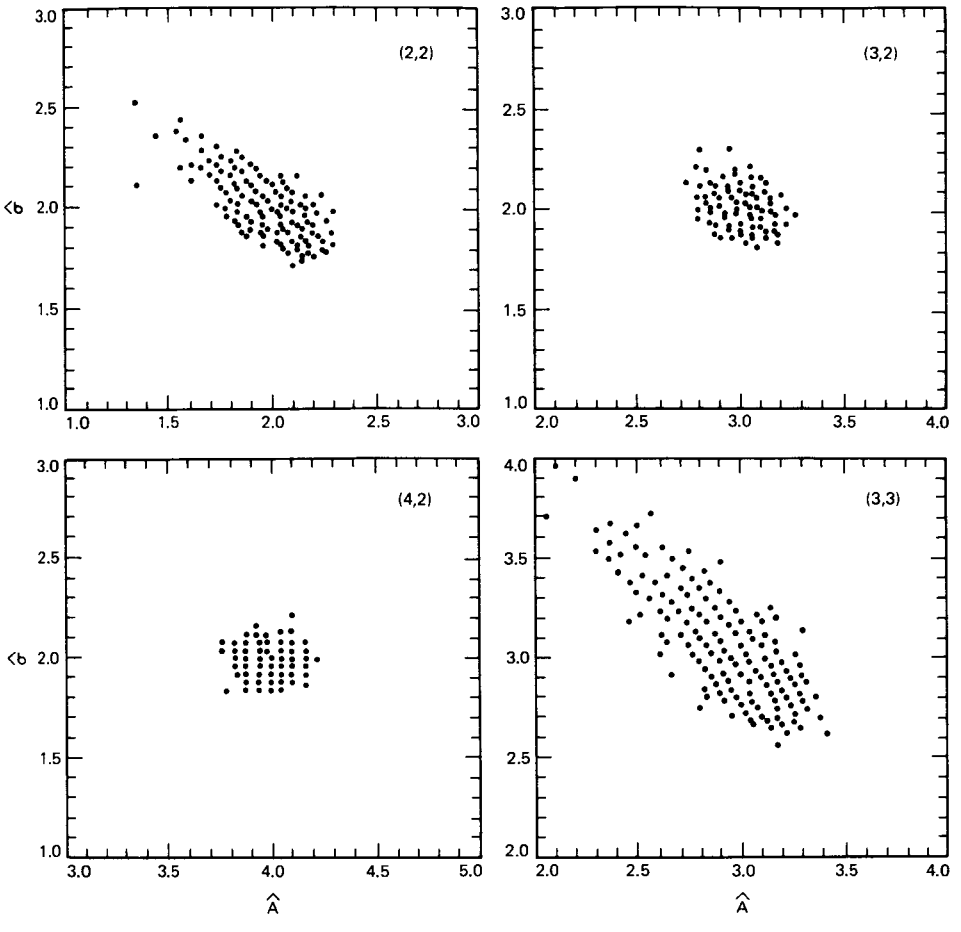

Fig. 2. Scatter diagrams at coordinates (A, σ)

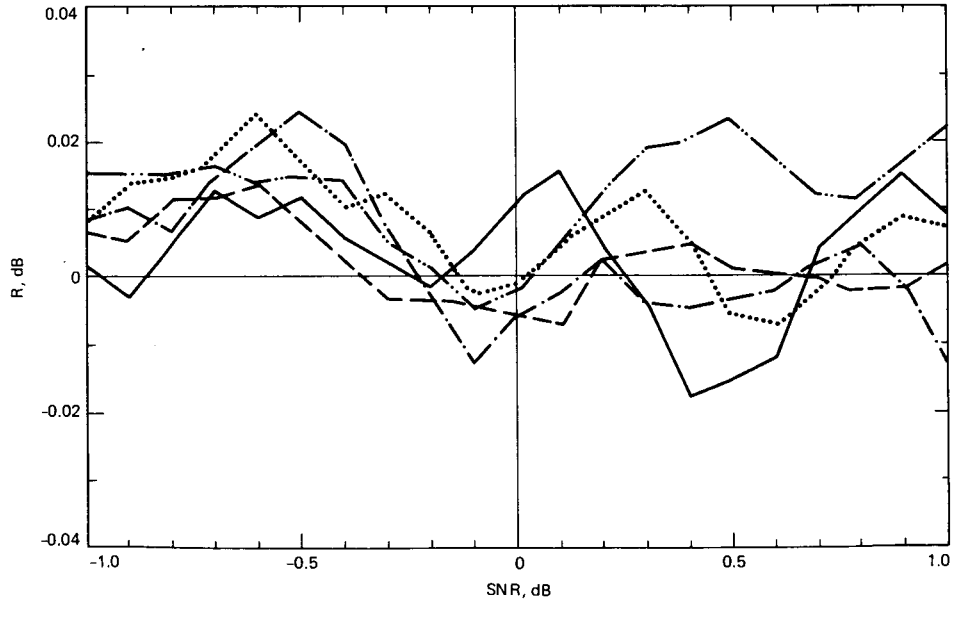

Fig. 3. The quantity R (dB) as a function of the true SNR

Appendix

In this appendix, formulas for the components of the Jacobian matrix C are derived, assuming four-bit quantization ($L = 4$). It is convenient to write the ℓth absolute moment of the quantized observable q as

$$\bar{\theta}_\ell = E(|q|^\ell) = \frac{1}{2}\sum_{j=-8}^{7} (|j|^\ell + |j+1|^\ell) f_j \qquad \text{(A-1)}$$

where

$$f_j = \int_{a_j}^{a_{j+1}} e^{-u^2/2}\, du/\sqrt{2\pi} \qquad \text{(A-2a)}$$

$$a_j = (j + A)/\sigma \qquad -7 \leq j \leq 7 \qquad \text{(A-2b)}$$

and $a_8 = +\infty, a_{-8} = -\infty$. Letting

$$\begin{aligned} e_j &= e^{-a_j^2/2}, \quad -7 \leq j \leq 7 \\ e_8 &= e_{-8} = 0 \end{aligned} \qquad \text{(A-3)}$$

it follows that

$$\frac{\partial f_j}{\partial A} = (e_{j+1} - e_j)/\sqrt{2\pi}\,\sigma \qquad \text{(A-4a)}$$

$$\frac{\partial f_j}{\partial \sigma} = [(j + A)\, e_j - (j + A + 1)\, e_{j+1}]/\sqrt{2\pi}\,\sigma^2 \qquad \text{(A-4B)}$$

Therefore, the components of the Jacobian C can be computed using

$$c_{\ell 1} = \frac{\partial \bar{\theta}_\ell}{\partial A} = \sum_{j=-8}^{7} \frac{1}{2}(|j|^\ell + |j+1|^\ell)\frac{\partial f_j}{\partial A} \qquad \text{(A-5a)}$$

$$c_{\ell 2} = \frac{\partial \bar{\theta}_\ell}{\partial \sigma} = \sum_{j=-8}^{7} \frac{1}{2}(|j|^\ell + |j+1|^\ell)\frac{\partial f_j}{\partial \sigma} \qquad \text{(A-5b)}$$

Having determined the components of C, C^{-1} can be computed and used in Eq. (25) to evaluate the covariance matrix of the estimation error.